

FINAL REPORT

Background Due to Cosmic Protons in
Gamma-Ray Telescopes

P-59

Prepared under

NA68-752

A Study of the Sensitivity of an Imaging Telescope (GRITS)
for High Energy Gamma-Ray Astronomy

Mason R. Yearian, Principal Investigator

(NASA-CR-186921) A STUDY OF THE SENSITIVITY
OF AN IMAGING TELESCOPE (GRITS) FOR HIGH
ENERGY GAMMA-RAY ASTRONOMY Final Report
(Stanford Univ.) 59 p

N90-29468

CSCL 20K

63/89

Unclas

0302490

Stanford University

W. W. Hansen Experimental Physics Laboratory
Stanford, California 94305

August 1990

Background Due to Cosmic Protons in Gamma-Ray Telescopes

Henry L. Edwards
Department of Physics
Stanford University
Stanford, CA 94309

June 6, 1990

Abstract

When a gamma-ray telescope is placed in Earth orbit, it is bombarded by a flux of cosmic protons much greater than the flux of interesting gammas. These protons can interact in the telescope's thermal shielding to produce detectable gamma rays, most of which are vetoed. Since the proton flux is so high, the unvetoed gamma rays constitute a significant background relative to some weak sources. This background increases the observing time required to pinpoint some sources and entirely obscures other sources. Although recent telescopes have been designed to minimize this background, its strength and spectral characteristics have not been previously calculated in detail. Monte Carlo calculations are presented here which characterize the strength, spectrum and other features of the cosmic proton background using FLUKA, a hadronic cascade program. Several gamma-ray telescopes including SAS-2, EGRET and GRITS are analyzed here, and their proton-induced backgrounds are characterized. In all cases, the backgrounds are either shown to be low relative to interesting signals or suggestions are made which would reduce the background sufficiently to leave the telescope unimpaired. In addition, several limiting cases are examined for comparison to previous estimates and calibration measurements.

Acknowledgements

First and foremost I would like to thank my parents who made this all possible. I would also like to thank E. Barrie Hughes and Robert Hofstadter for their guidance in my research, as well as Y. C. Lin and Pat Nolan for always being there to answer my questions. Special thanks go out to Barbara Dillard Marilyn Bailey, and Gerda Wilson, who run the place, and Mason Yearian for his advice and encouragement about my thesis. The advice from and information provided by David Koch, Carl Fichtel and Bob Hartman from NASA are much appreciated, as are the consultations of Pertti Aarnio of the Helsinki Institute of Technology and Ralph Nelson of SLAC. I also wish to express my gratitude to Thomas Bontly for his invaluable assistance in editing, revising and regressing.

Contents

1	Introduction	2
1.1	Advantages of Gamma-Ray Astronomy	2
1.2	Gamma-Ray Telescopes	4
1.3	Background Problem	6
1.4	Gamma-Ray Sources	8
1.5	Effects of Cosmic Background	9
1.6	A Treatment of the Problem	10
2	Cosmic Ray Physics	11
2.1	The Origins of Cosmic Rays	11
2.2	Cosmic Protons	12
2.3	The Solar Wind and Cosmic Rays	13
2.4	The Terrestrial Magnetic Field	13
2.5	Cosmic Proton Spectrum in Orbit	16
3	Calculating the Background	18
3.1	Extragalactic Diffuse Source	18
3.2	Outline of the Calculation	19
3.3	Mathematical Methods	21
3.4	The FLUKA Software Package	22
3.5	The Actual Calculation	23
3.5.1	Cosmic-Proton Background	23
3.5.2	Extragalactic Diffuse Source	24
3.6	Statistical Error Estimate	25
3.7	Discussion of Assumptions	26

4	Several Case Studies	27
4.1	The SAS-2 Telescope	28
4.1.1	The Telescope Model	28
4.1.2	The Shield Model	29
4.1.3	Extragalactic Diffuse Count Rate	29
4.1.4	Background Estimate	30
4.2	The EGRET Telescope	31
4.2.1	The Telescope Model	32
4.2.2	The Shield Model	32
4.2.3	Extragalactic Diffuse Count Rate	33
4.2.4	Background Estimate	33
4.3	The GRITS Telescope	34
4.3.1	Telescope and Tank Wall Models	34
4.3.2	Three Possible Configurations	35
4.3.3	Extragalactic Diffuse Count Rate	36
4.3.4	Background Estimate	36
4.4	Beam Test of EGRET	37
4.4.1	Beam Test Model	38
4.4.2	Estimated Rate of Acceptable Gamma Rays	39
5	Conclusions and Context	40
5.1	The Advance of Gamma-Ray Astronomy	40
5.2	Applicability to Similar Fields	42
5.3	Future Work in Gamma-Ray Astronomy	43
A	Pictures of the Real Telescopes	44
B	Background Spectrum from a GRITS Model	45
C	Summary of Background Estimates	46

Chapter 1

Introduction

For many years, man has looked to the sky in an attempt to understand his world. The ancients saw their heroes and deities immortalized in heavenly forms while astrologers followed the stars to create calendars and predict the future. More recently, scientists have sought a glimpse of phenomena too hot, cold, big, dense or fast to be observed within the confines of our relatively hospitable Earth. Newton used Kepler's observations about planetary motion to formulate a theory of mechanics which was not successfully challenged until this century. Hubble observed the recession of distant galaxies and inferred the expansion of the universe, a critical piece in the puzzle of cosmology. Current attempts to unify the disparate theories of quantum mechanics and general relativity often appeal to such events as the big bang and black holes in which the effects of both theories must be important. The field of astronomy, therefore, has been, and still is, quite important in providing information about the character of nature.

1.1 Advantages of Gamma-Ray Astronomy

Newton knew that light came in many colors, and ascertained with the use of a simple prism that these colors did not act identically — some colors were bent more by the prism than others. In the late nineteenth century, it was found that light is actually composed of many more “colors” than could be seen, and that these

colors of light exhibited an astounding array of different behaviors. This variety can be explained by the fact that each color of light has an energy associated with it, and that "bluer" light carries more energy while "redder" light carries less. Light of high energy interacts in high-energy phenomena. The very high-energy light at the extreme blue end of the spectrum is called gamma radiation.

The vast majority of astronomical observations have naturally used visible light. Since different colors of light have different properties, however, one suspects that different processes will interact with or produce different colors of light. This is in fact the case, so much modern astronomy has explored the sky in these different colors. Furthermore, different colors of light are presumably affected by slight interactions with interstellar matter in varying degrees. They therefore differ in their abilities to accurately represent their point and mechanism of origin. The color of light considered from this point on is that of the highest energy, gamma radiation.

Gamma rays are the most energetic color of light so they are deflected far less by interstellar gases than are light rays of other colors. For instance, gas clouds in the center of our Milky Way galaxy obscure its structure in visible regions, but it is thought that gamma rays have enough energy to penetrate these dense regions, giving clues to the processes taking place therein. In addition, since gamma rays are so energetic, they are given off by very energetic processes. One general trend in experimental physics has been to explore higher and higher energies, and gamma ray sources may provide us with glimpses of new physics at energies unattainable on the Earth.

While the high energy of gamma rays makes them valuable as a probe for cloudy sources and new phenomena, it also enables them to interact with atoms and produce pairs of electrons and positrons. When a gamma ray hits the Earth's atmosphere, it interacts in this way, producing a cascade of other particles. For this reason, gamma rays are unable to penetrate the Earth's atmosphere unperturbed. It is therefore necessary to observe them in space, outside the absorbing effects of the air.

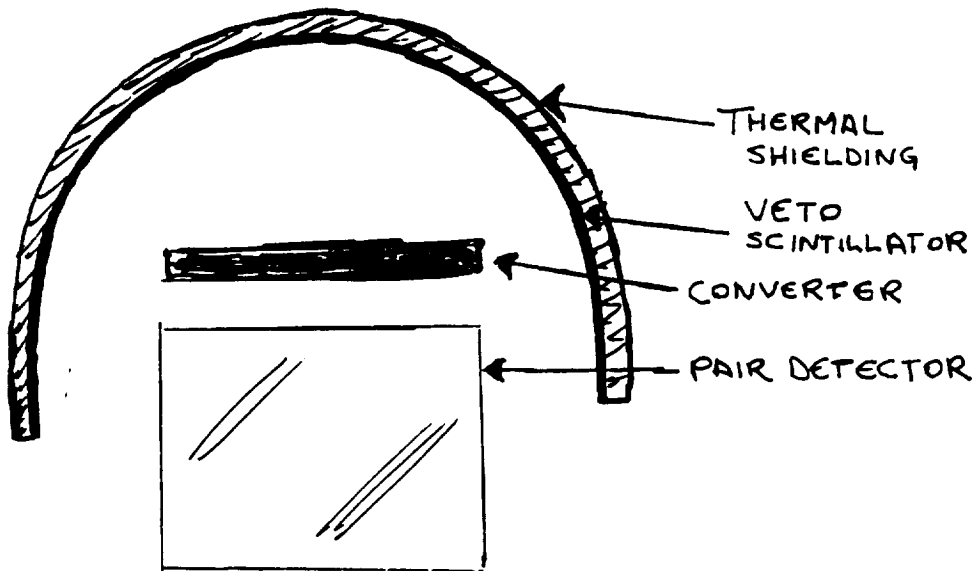


Figure 1.1: The basic design of a gamma-ray telescope

1.2 Gamma-Ray Telescopes

Since gamma rays are, by definition, not visible, gamma-ray telescopes must differ markedly in design from conventional visible light telescopes. For instance, a mirror does not reflect a gamma ray; usually it will not even stop a gamma ray. A gamma-ray telescope is generally not even recognizable as a telescope on a casual inspection, as can be seen in figure 1.1.

All gamma-ray telescopes flown so far have operated on the same basic principle. That is, gamma rays interact with matter to produce a pair, an electron and a positron. Since these have charge (the electron negative and the positron positive), they interact strongly with matter and are easily detected. The main component of a gamma-ray telescope is a detector which can measure the trajectories of this pair. Some telescopes use a spark chamber, which simply tracks the paths of ionized gas that the electron and the positron leave behind — it employs an effect similar to lightning. Others use what is called a Cerenkov detector, which works on the principle that the speed of light is slower in a

dense medium than it is in the vacuum. A quickly moving electron or positron will seem to move faster than light in the medium, creating a light 'cone' about the trajectory of the particle which is analogous to the shock wave created when a supersonic jet crosses the sound barrier. This light cone is detected for the electron and the positron to determine the trajectory of the original gamma ray. These two detector schemes are relatively complex, but the basic idea is this: a gamma ray impinges on the telescope, where it encounters a certain amount of inert material, called the converter. Some of the gamma rays interact in this converter, producing an electron-positron pair, which is then detected by one of the above schemes, and once their trajectories are determined, that of the gamma ray can be estimated.

In addition to determining the gamma ray's trajectory, some telescopes can also measure the gamma ray's energy. There are two ways in which this can be done. One way that any gamma-ray telescope can roughly estimate the gamma-ray's energy is by measuring the angle between the electron and positron after creation. A high-energy gamma ray produces a pair with a small angular separation, and a lower-energy gamma ray produces a pair with a large angular separation. This method is only approximate, however, because the measurement of the angular separation is generally imprecise. Telescopes such as GRITS¹ estimate the gamma ray's energy E in this way, and the value of E has been shown theoretically to have a statistical error of one hundred percent [1]. As will be discussed momentarily, it is not necessary that all gamma-ray telescopes measure a source's energy spectrum precisely.

To obtain an accurate measurement of a gamma ray's energy, a calorimeter can be placed at the downstream end of the telescope². The calorimeter absorbs the pair and measures their total energy. Since the pair detectors absorb a small and predictable amount of the pair's energy, the energy of the incident gamma ray can be determined fairly accurately. The EGRET³ telescope employs a Sodium Iodide scintillating calorimeter.

¹A proposed NASA telescope which would employ the Cerenkov pair detection scheme. The telescope would be housed in a discarded Space Shuttle external fuel tank

²cf. figure 1.1

³to be launched by NASA in 1990. This telescope uses the spark chamber pair detector scheme

There are several general features of the telescopes that should be noted. First, when a gamma ray encounters matter, the probability that it will interact in the matter to produce a pair is roughly proportional to the amount of matter that it sees. This amount is usually expressed in gm/cm^2 and is found by multiplying the density of the material (in gm/cm^3) by the distance traversed in the material (in cm). Since the chances of detecting the gamma ray depend directly on the probability that it produces a detectable pair, the rate of detection must depend directly on the amount of matter in the converter, so a heavy gamma-ray telescope will be able to detect more gamma rays in a given time than a light one will.

As with light telescopes, the detection rate is proportional to the area of the detector since a larger number of gamma rays will happen to fall on a larger area. The rate at which the gamma rays are observed is then proportional to both the detector's active area or aperture and its converter thickness. A heavier, broader telescope can observe more gamma rays in a given time than a lighter, smaller one.

The original gamma-ray telescopes were small and carried by balloons. Later, small telescopes were launched on satellites. The EGRET telescope is larger and heavier, and the proposed GRITS telescope will be enormous since it will occupy the spent external fuel tank of a space shuttle. Thus the trend in gamma-ray astronomy is to the larger and heavier telescopes which are capable of detecting progressively higher rates of gamma rays.

1.3 Background Problem

A gamma-ray telescope must be placed in orbit to avoid the absorbing effects of the Earth's atmosphere. This absorption is nearly complete for many different kinds of radiation, so that what reaches us on the ground is just a small fraction of the radiation flying about through space. In addition to all of the different colors of light, there are subatomic particles and nuclei from outside of the solar system bombarding an orbiting telescope. These particles are called cosmic rays. By far the most important component of the

cosmic rays is the proton; the next most common is the helium nucleus, these being about ten times less common than the protons. The protons are far more numerous than gamma rays from interesting sources.

Any satellite must have some sort of shielding to protect it from the micrometeorite impacts and the extremes of temperature to which it is exposed in orbit. This shielding inadvertently provides matter in which the cosmic-ray protons can interact. Some of these interactions are nuclear, i.e. the protons interact with the nuclei of the atoms in the shield. The protons are often extremely energetic so that these interactions produce many different types of particles. One type of particle that is produced is called a π^0 meson⁴. This is an unstable particle, decaying in about 10^{-16} seconds — practically instantaneously — into a pair of gamma rays. These gamma rays are sometimes detected by the telescope, and thus constitute a source of background.

A partial cure for this cosmic proton background is afforded by placing a charged particle detector called a scintillator dome directly inside the thermal shielding⁵. When a cosmic proton interacts in the shield, many particles are produced, some of which may be charged. If any of these charged particles are incident on the dome, they will trigger it. The telescope's control system can then veto any gamma ray detected concurrently. Thus the scintillator is called the veto dome. Since most of the protons' interactions produce charged secondaries, the vast majority of the detectable gammas will be vetoed.

On a first glance, it seems that the veto dome solves the background problem. The fact is, though, that there are so many more cosmic ray protons than there are interesting gamma rays bombarding the telescope that the unvetoes background rate can be comparable to the rate of source gamma rays. For some early telescopes, in fact, this problem was so serious that the background overwhelmed many interesting sources.

⁴pronounced pi-not meson

⁵cf. figure 1.1

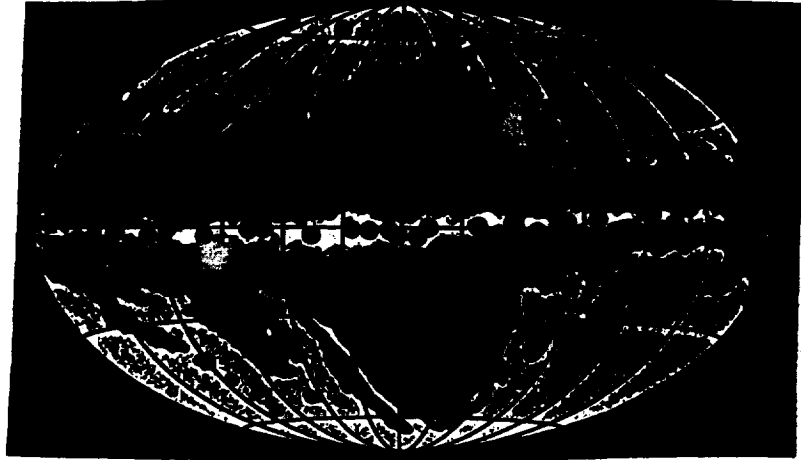


Figure 1.2: Gamma-ray map of the sky made by SAS-2.

1.4 Gamma-Ray Sources

Several telescopes have been launched which have taken surveys of the sky in the gamma-ray region. SAS-2⁶ and COS-B⁷ were launched in the 1970's and are the two most important. Each surveyed the gamma-ray sky and located a number of gamma-ray sources. The SAS-2 map is shown in figure 1.2. There are two types of gamma-ray sources: point and diffuse. A point source is just what it sounds like — a source from which all of the gamma rays detected originate in exactly the same place. Such sources are believed to be high energy stellar phenomena such as black holes, supernovae, pulsars and quasars, among others. The previous surveys have revealed 25 to 30 pointlike sources, but the telescopes were unable to resolve most of them sufficiently to identify them with particular visible sources. Two pulsars, the Crab and the Vela, have tentatively been identified as gamma-ray sources because the intensity of the light emitted by a pulsar varies in time, so the gamma-ray count rate could be checked for this kind of variation. For pointlike sources which do not vary in time, tremendous angular resolution is required to identify them with visible sources, especially in crowded regions of the sky. Angular resolution is a function of the number of gamma rays detected, so a large telescope

⁶NASA

⁷European Space Agency, ESA

like GRITS is ideal for locating them. Once they have been identified with sources in other wavelengths, telescopes with limited angular resolution but excellent spectral resolution can be used to further characterize the physics of the sources. This is the reason that GRITS does not need sharp energy resolution.

Diffuse sources seem to come uniformly from large regions. There is diffuse gamma radiation coming from the whole galactic plane which is believed to be due to the interaction of cosmic-ray protons with the interstellar medium. Another source of diffuse gamma rays seems to be the universe itself — these come from outside of the Milky Way. This source is called the extragalactic diffuse source⁸, and it is quite important since it is the weakest of the interesting sources. It is therefore used as a benchmark against which to judge various other signals, including backgrounds.

1.5 Effects of Cosmic Background

The background due to cosmic protons appears in a telescope as a diffuse signal, since the protons are isotropic. If this background is too high, therefore, it is indistinguishable from a weak source — both produce similar signals. There is then no direct way to determine whether a particular telescope is measuring a true diffuse source or a proton-induced background.

When a point source is surrounded by a halo of diffuse background, it can still be located, but over a longer observing time since statistical fluctuations will eventually average themselves out. A telescope with a higher background rate will then take longer to locate sources and so will be unable to observe as many sources (or pinpoint them as well) as a telescope with a lower background.

The cosmic proton background then causes two major problems. First, one cannot be certain if the extragalactic diffuse source is a true source. Second, a telescope with high background will not be able to catalogue as much of the sky as one with low background.

It should be mentioned that, although a direct measurement of the extragalactic diffuse source is not feasible when the cosmic

⁸cf. figure 1.2. The extragalactic region is that not in the galactic plane, i.e. the upper and lower regions of the map.

proton background is an unknown, reliable estimates have been made by Dave Thompson and Carl Fichtel [8].

1.6 A Treatment of the Problem

The most significant hurdle to overcome in treating this background problem is the calculation of its rate for a particular satellite design. If the calculation were simple, then the rate could be calculated and accounted for in any measurement. As was mentioned above, however, the vast majority of interacting protons produce charged secondaries, so the vast majority of potential background gamma rays are vetoed. In addition, the physics involved in a nuclear reaction is quite complex. Both of these facts indicate that a simple "back-of-the-envelope" calculation will not suffice to predict the background rate, although a simplified physical argument will be given later to augment a more detailed calculation.

With access to powerful computers at SLAC and data on cosmic ray composition, it has proven possible to predict the background rate for several gamma-ray telescopes. This prediction can be compared in limiting cases to other measurements to verify its accuracy.

Chapter 2

Cosmic Ray Physics

The Solar system is perpetually being bombarded by cosmic rays. Cosmic rays have been observed to possess a wide range of energies. Extensive measurements of the cosmic rays' energetic, or spectral, characteristics have been performed. Balloon-borne detectors have measured the cosmic ray fluxes at low and intermediate energies, and ground detectors have observed Extensive Air Showers (AIS's) caused by very high-energy cosmic rays.

2.1 The Origins of Cosmic Rays

The origin of cosmic-ray particles is not well understood since most of them carry very little information about their beginning. For instance, protons (and most other cosmic rays, for that matter) are charged, so their paths are bent by magnetic fields. When we observe these protons, therefore, their trajectories may have little to do with their points of origin. Another result of their charge is that they interact with nearly anything that they encounter, so their energies may be unrelated to their original energies as well.

Cosmic rays have been observed to have high energies. If they were being produced by some system in thermal equilibrium, such as a star, their energy would be of the same order of magnitude as the thermal energy of that system. For instance, cosmic rays have been observed at energies of 100 TeV (trillion electron volts). The thermal energy of a system at temperature T is about $E_{\text{thermal}} \approx kT$

so that the temperature of the production mechanism must be about a million trillion degrees Kelvin, the temperature of the universe a tiny fraction of a second after the big bang. Cosmic rays have been observed with energies greater than one 100 Million TeV [4], so they obviously cannot all have simply been thrown off by hot objects; there are too few hot objects around to account for the observed flux, and the hot objects that do exist are too cool to produce observable fluxes of such high energy cosmic rays.

There are a number of physical mechanisms which can accelerate charged particles to very high energies. Some candidates are supernova explosions such as 1987A, migrating magnetic fields in interstellar space, and 'metagalactic' mechanisms. After a cosmic-ray particle is produced by one of these mechanisms, it would travel through space, encountering gases and other matter, and would hence undergo a diffusion process modifying its energy and direction. This combination of acceleration and diffusion process is supported well by observations of cosmic-ray spectral characteristics, although it is difficult to choose a specific mechanism of acceleration [5].

2.2 Cosmic Protons

The most important component of the cosmic-ray flux is composed of protons, since these are far more numerous than the other components are. The spectrum of the proton flux is approximated well by an equation called a power law. Theory predicts that if cosmic rays are in fact accelerated and then subjected to a diffusion, their spectra will be described by a power law, in support of the foregoing mechanisms of cosmic-ray production [7].

The spectrum of the proton flux has been fit to the equation

$$J_p E = 1.18 \times (E + 3.3)^{-1.7} \text{ protons/cm}^2\text{s sr} \quad (2.1)$$

This is an integral flux, meaning that there is a flux of J_p protons (per second, per square centimeter, per steradian of solid angle) with energy over E , in GeV (billions of electron volts). This is, theoretically at least, the flux of cosmic-ray protons incident on the outer reaches of our solar system. The flux of interest is, of

course, that in a typical Earth orbit, so the effects of the solar wind and the Earth's magnetic field must be considered in obtaining a cosmic-ray flux useful in calculating cosmic-ray background.

2.3 The Solar Wind and Cosmic Rays

As a cosmic-ray proton flies toward the Sun, the solar wind streams past, occasionally interacting with it. This interaction has the overall effect of exerting a pressure on the cosmic rays such that low-energy cosmic rays are blown back in their path, leaving only the higher energy portion of the flux. The solar wind thus truncates the cosmic proton spectrum; the level of truncation increases nearer the Sun.

Cosmic rays with momenta lower than a few GeV/c are unable to approach as close as one Astronomical Unit¹ to the Sun, so the cosmic-ray flux at the Earth's orbit is truncated at a few GeV/c. The exact level depends on the intensity of the solar wind, which in turn depends on the level of solar activity. During a period of minimum solar activity, this truncation occurs for protons with a momentum of less than 1 GeV/c, and during solar maximum, protons with momenta up to 5 GeV/c are swept away by the solar wind. This solar modulation of the cosmic proton flux determines the cosmic-ray intensity on the moon, but for a low equatorial orbit about the Earth, the terrestrial magnetic field blocks the cosmic rays further. Thought has been given to the possibility of a moon-based gamma-ray telescope, but its design has not been agreed upon; a calculation of its cosmic-proton background is, therefore, not included here.

2.4 The Terrestrial Magnetic Field

The shape of the Earth's magnetic field closely resembles the shape of a dipole which is aligned fairly close to the Earth's axis of rotation. The field lines extend from the north pole to the south pole as in figure 2.1. Charged particles tend to spiral around magnetic

¹Earth's orbit, in other words

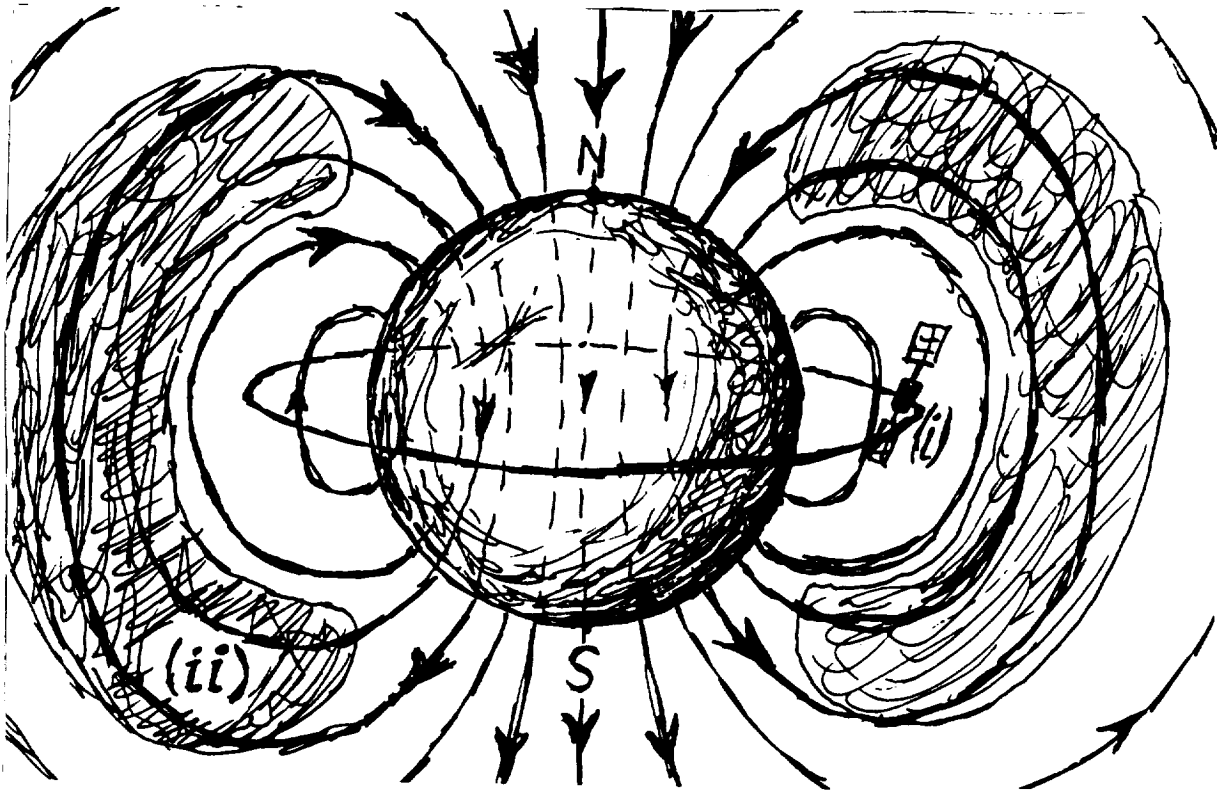


Figure 2.1: The Earth's magnetic field. (i) A low orbit. (ii) Van Allen radiation belt

field lines, so cosmic protons without enough energy will curve back out into space. Incidentally, some particles (mainly electrons since they are so light) are actually trapped in spiral paths around the lines, and bounce back and forth between the north and south poles in what are called the Van Allen radiation belts. In periods of extreme solar activity such as flares, these trapped particles are pushed toward the poles by the same type of solar wind pressure that pushes low-energy cosmic rays out of the solar system. The particles which are forced out of the radiation belts into the atmosphere near the poles interact with air molecules and give off a glow which is known as the Aurora Borealis (Northern Lights) and the Aurora Australis (Southern Lights). The Van Allen belts are lobe-shaped, leaving a large volume surrounding the equator relatively free of the trapped radiation. This volume is obviously a good place to put a gamma-ray telescope.

Near the equator, a cosmic proton has to pass more field lines than it does near the poles, so it is harder for a cosmic proton to penetrate to the equatorial regions of the earth than it is to

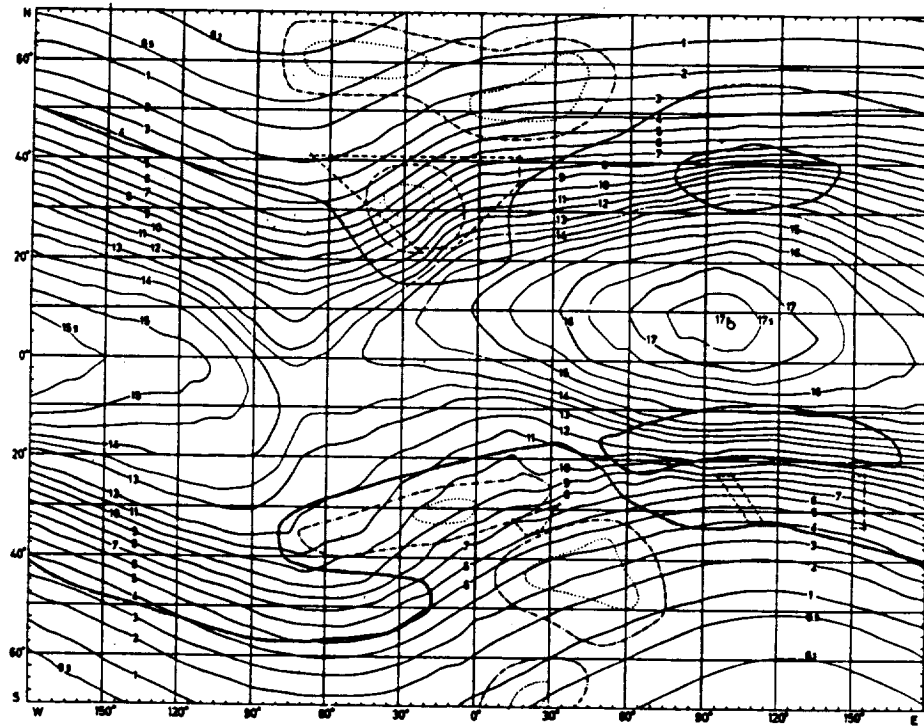


Figure 2.2: Map of threshold rigidities over the Earth's surface. Reproduced from Sandstrom, *Cosmic Ray Physics*. New York, Wiley and Sons (1965) p. 125

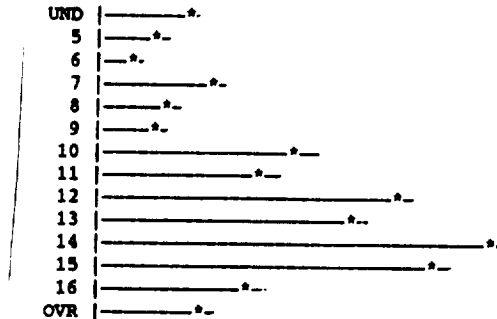


Figure 2.3: Threshold rigidity distribution averaged over the GRO orbit, inclined 30 degrees with respect to the equator. The rigidity is in GeV/c

reach the poles. This phenomenon, called the geomagnetic effect, requires that a proton have a momentum which is greater than a certain value, called the geomagnetic threshold rigidity, to reach that point on the Earth. This has been measured, and its values across the globe can be plotted on a map, as in figure 2.2. Rigidity is defined for a more general class of particles by the size of the circular orbit they execute in a fixed magnetic field, but for protons, it is numerically equal to the linear momentum [6].

For a low orbit of about 300 miles, the threshold rigidity is approximately the same as it is at the Earth's surface. The Earth's radius is about 4000 miles, and a dipole field drops in intensity as the cube of the distance, so the magnetic field at 300 miles is about $(3700/4000)^3 \approx 80$ percent of that at sea level. As can be seen in figure 2.2, the threshold rigidity varies by amounts far greater than twenty percent, so the threshold distribution in a low orbit can be assumed to be similar to that at the Earth's surface.

2.5 Cosmic Proton Spectrum in Orbit

The gamma-ray telescope for which the most detailed background calculations have been done is the EGRET telescope, scheduled to fly on the Gamma Ray Observatory (GRO) in late 1990. This satellite will have a low orbit inclined at approximately 30 degrees

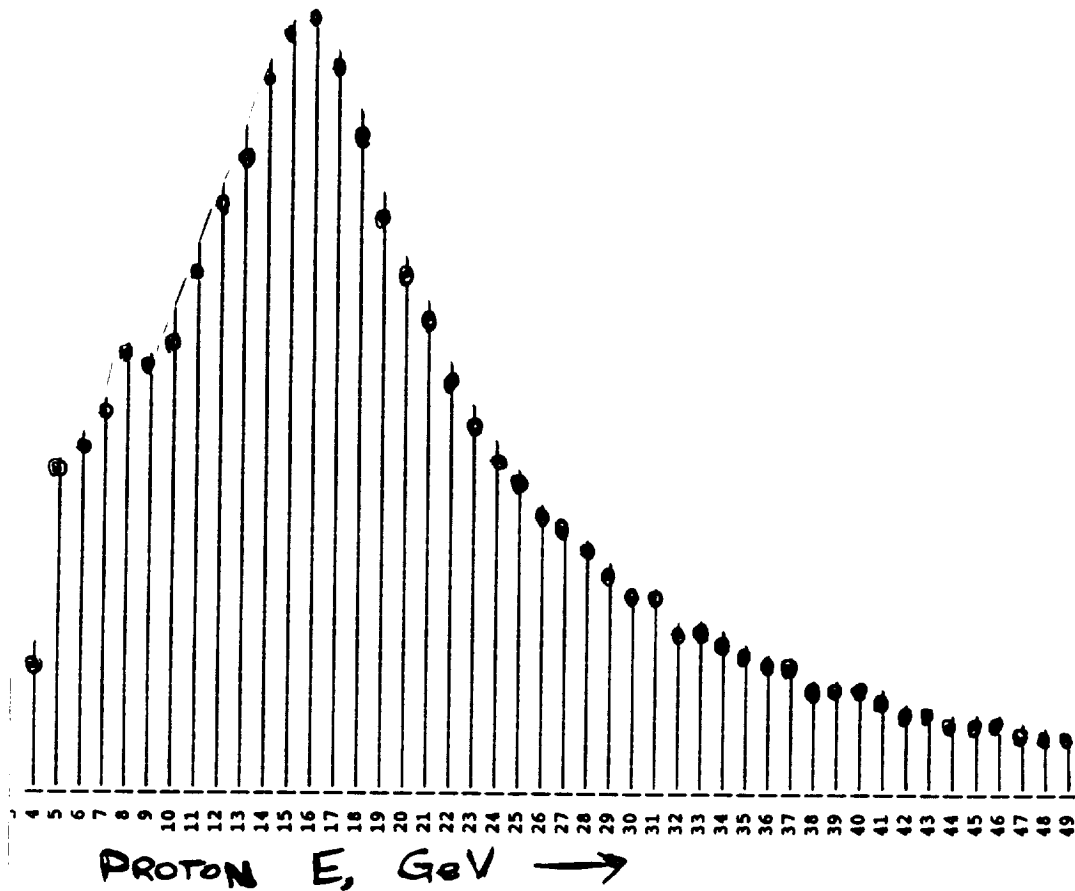


Figure 2.4: Differential spectrum of the cosmic protons in GRO's low-Earth orbit. The integral of this spectrum is the total flux of cosmic protons in this orbit, or 0.01219 protons/cm²sr

to the geographic equator, varying between 30 degrees north and south latitude over its orbits. A threshold rigidity distribution, figure 2.3, can be calculated by averaging the thresholds at different places on the orbit with respect to the amount of time spent over those regions.

At each point of the orbit, the Earth's magnetic field truncates the primary cosmic proton spectrum (Equation 2.1). Then this spectrum, too, can be averaged over the satellite's orbit, as is given in figure 2.4 in differential form. The integral of the spectrum corresponds to the absolute rate at which cosmic protons would expose a square centimeter from one steradian of view. It is important to note that this spectrum is specific to GRO's orbit.

Chapter 3

Calculating the Background

When treating an instrument background, it is important to determine first how it should be quantified. In other words, what units do we use? As was mentioned on page 9, the proton background appears to the telescope as a diffuse signal. Hence, it makes sense to state the background in the same units used to quantify a diffuse flux.

A diffuse flux is expressed in terms of the number incident gamma rays per second on a certain area from a certain direction, i.e. amount of solid angle. A full sphere subtends a solid angle of 4π steradians with respect to its center. The specific units generally used to express fluxes of gamma rays are photons/(cm²s sr). The cosmic-ray proton background will then be expressed in terms of the diffuse flux that the telescope detects.

3.1 Extragalactic Diffuse Source

The extragalactic diffuse source is what is seen when looking out of the galaxy. In gamma-ray astronomy, this is the weakest interesting diffuse source, so it is useful as a benchmark against which to judge potential backgrounds. Like many things in astrophysics, its spectrum fits well to a power law. The integral form of its

spectrum is

$$J_{EG} = 6.7 \times 10^{-3} E^{-1.35} \text{ gammas/cm}^2\text{s sr} \quad (3.1)$$

Thus from one steradian of view, J_{eg} gamma rays of energy greater than E (this time in MeV or millions of electron volts) impinge on one square centimeter in one second.

The cosmic proton background appears to the telescope as a diffuse flux like the extragalactic source, so the background flux may also be expressed as a fraction of the extragalactic flux over some energy.

3.2 Outline of the Calculation

In principle, the calculation is quite straightforward. One imagines exposing a telescope to a flux of cosmic-ray protons. A certain fraction of these protons undergo nuclear interactions in the thermal shield, some of which which create a π^0 which decays into two gammas, a few of which will be detected. Of the tiny fraction of incident cosmic protons which actually produce a detectable gamma ray, the overwhelming majority will also produce a number of charged particles, some of which will trigger the veto dome¹. Therefore only the tiniest fraction of the incident protons will produce a detectable gamma ray which is not accompanied by a veto signal from the scintillator dome.

The calculation can be posed as a multi-dimensional integral where the dimensions might be chosen, for instance, as telescope aperture, solid angle, proton energy, and a number of 'internal dimensions' which reflect the physics of the nuclear interaction in the shield and then the gamma detection in the telescope. Since the chance that a given proton will produce a background gamma has already been shown to be quite low, this integral could be described as 'terribly slowly convergent'. A numerical integration is quite demanding on even the most powerful computers, and after hundreds of hours of CPU-time on the SLAC computers the statistical errors on some background estimates were still as high as 50 percent.

¹see figure 1.1 for the geometry of the telescope

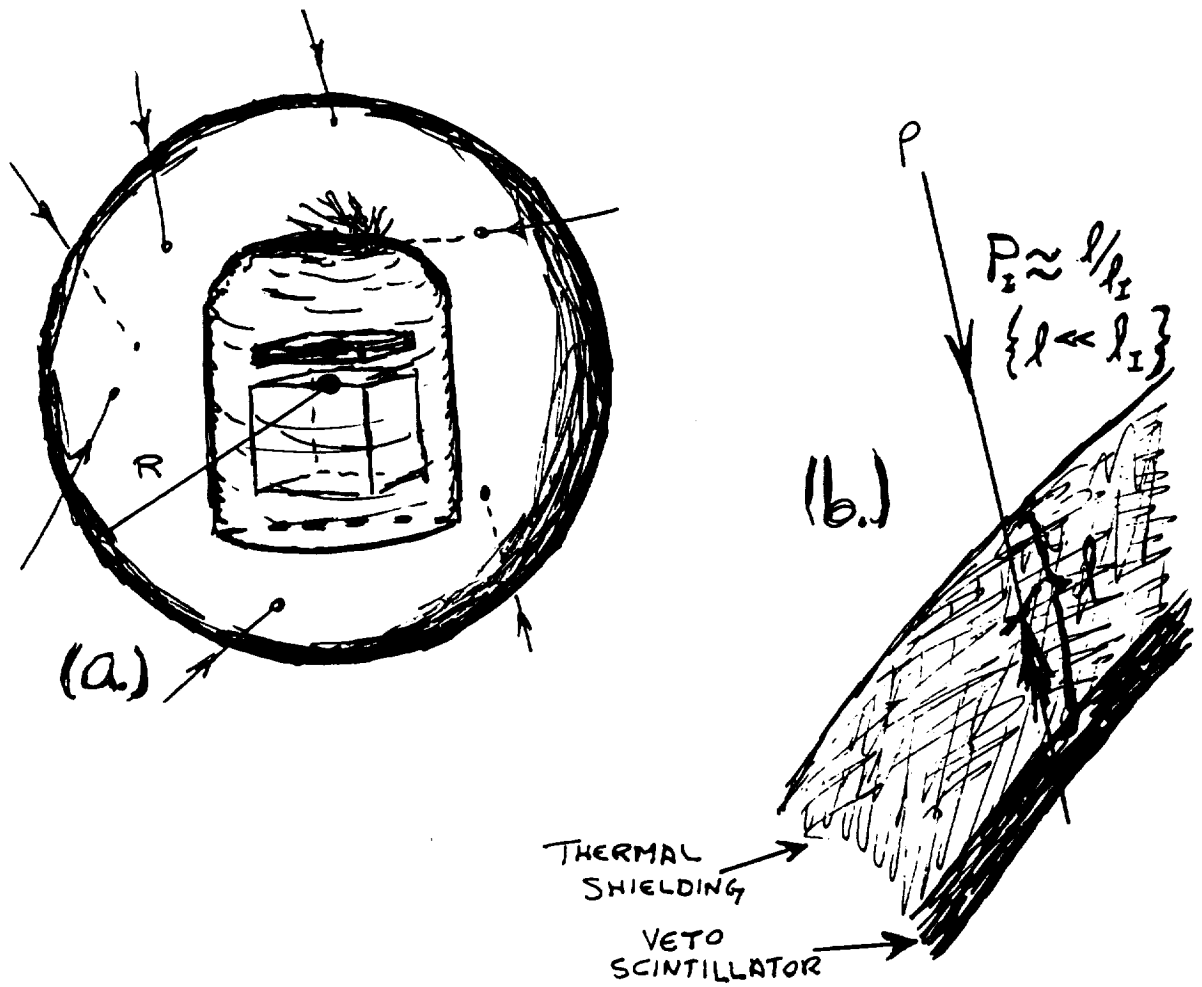


Figure 3.1: a. An imaginary sphere is placed around a gamma-ray telescope and exposed to a given flux of protons. b. For a proton trajectory which intersects the shield, there is a certain probability that the proton will experience a nuclear interaction along its pathlength which is proportional to the amount of material that the proton 'sees'.

3.3 Mathematical Methods

Specifically, one imagines a sphere that entirely encloses the telescope under consideration². We assume that the flux of cosmic-ray protons is completely isotropic and so exposes all of this sphere uniformly. Since the telescope is in orbit, it will experience some average flux of cosmic protons. For simplicity, this is taken to be that of the GRO 300-mile, 30 degree orbit. The total proton flux is given by the integral of the spectrum in figure 2.4, or

$$\Phi_P = 0.01219 \text{ protons/cm}^2\text{s sr} \quad (3.2)$$

The sphere that is chosen will have some radius R , and hence an exposed surface area of $4\pi R^2$. Since the cosmic proton flux is assumed to be isotropic, each element of area on this sphere is exposed by 2π sr solid angle of flux. The sphere is therefore illuminated at a rate of

$$(\Phi)(4\pi (R \text{ cm})^2)(2\pi \text{ sr}) = 0.9625 R^2 \text{ protons/s} \quad (3.3)$$

When a proton traverses material, there is a certain chance per unit length that it will undergo a nuclear interaction³. If, therefore, many protons illuminate a piece of material, there will be a certain length after which a significant portion⁴ will have interacted, called the interaction length l_I . The probability m that a proton has interacted in the material after a distance l is given by an exponential distribution

$$m = (1 - e^{-(l/l_I)}) \quad (3.4)$$

so that for $l = l_I$, $m = 1 - e^{(-1)} \approx 0.6321$. The most obvious units for l are cm, since it is a measure of the penetrating power of the protons. The truly fundamental quantity is actually, however, the number of nuclei that the proton sees in l , which is proportional to the total amount of matter in a unit area. The most convenient units for the interaction length are the product of the material's density and the actual distance, or $(\text{gm/cm}^3)(\text{cm}) = \text{gm/cm}^2$. The

²see figure 3.1a for the geometry

³see figure 3.1b

⁴more exactly $1-1/e=63.21$ percent

materials that compose the shields of the telescopes considered here are organic plastics for which $l_I \approx 55 \text{ gm/cm}^2$ and aluminum for which $l_I \approx 70 \text{ gm/cm}^2$. Since the densities of the shielding materials is always less than a few gm/cm^3 and the actual thicknesses are just a few cm, all possible path-lengths in the shielding material are much smaller than the interaction length so that the interaction probability 3.4 can be Taylor-expanded to

$$m \approx (1 - (1 - l/l_I)) = l/l_I \quad (3.5)$$

The sphere is exposed to a certain flux of isotropic protons. For a given trajectory, it can be determined geometrically whether the trajectory intersects the telescope's shield. If it does, then the proton will intersect a certain path length in the shield and have a probability⁵ m of interacting in the shield.

To calculate the behaviour of the protons that do interact in the shield requires a very wide range of physical laws and relations. Computer programs exist which simulate the behaviour of elementary particles as they traverse and interact in matter of some composition and geometry. One of these programs must be used to calculate the probability that the proton will produce an unvetoes, detectable gamma ray.

3.4 The FLUKA Software Package

The program, or rather set of programs, chosen to follow proton interactions in the shield is called FLUKA and was written over a period of years at CERN [9]. It calculates hadronic cascades in matter and was originally motivated by calorimetry predictions and health physics concerns, but its calculating power was soon realized for the prediction and interpretation of high-energy physics experiments.

FLUKA's internal workings are taken here as a physicist's 'black box', but a brief explanation is instructive. All of the above calculations take place in a subroutine which FLUKA calls SOURCE. This routine tells FLUKA the trajectory and energy of a particular cosmic proton, and FLUKA simulates the behavior of this proton

⁵the exact form 3.4 is used in the calculation

in the shield. FLUKA then produces a record of particles produced and their characteristics and interactions which are in turn analyzed by a separate analysis package. The analysis package decides whether or not a gamma ray was detected and whether or not the veto was triggered. It then recreates any events which qualify as background events⁶. The SOURCE routine and the analysis package are specific to this background calculation.

3.5 The Actual Calculation

In practice, individual protons are chosen incident on the sphere⁷ so both their positions and trajectories are uniformly random, the positions over the area of the sphere and the trajectories over the 2π steradian solid angle exposing each point. The protons' energies are chosen randomly from the cosmic proton spectrum in figure 2.4. This method of picking the independent variables of an integral randomly according to given distributions is called 'monte carlo' integration.

3.5.1 Cosmic-Proton Background

For a given simulation, N protons are selected in the above manner. The trajectory of each is checked, and a certain subset of the original N protons are found to intersect the telescope's shield. Since the probability that a given proton interacts in the shield is very small⁸ Therefore, if the one were to try different trajectories until one happened to interact in the shield (as actually tends to happen in nature), the computation would be intractable. To avoid this situation, the following statistical method is used.

For each proton's trajectory in the shield, there is a certain probability m that it interacts. If it does not interact, it either triggers the veto scintillator or simply passes through the shield for grazing trajectories. These cases are irrelevant for the purposes of the background calculation since neither can produce a background

⁶i.e. gamma detected with no charged particles triggering the veto scintillator.

⁷see figure 3.1a

⁸cf. equation 3.5, most protons either pass through the shield (grazing trajectories) or trigger the veto scintillator. The probability is generally a fraction of a percent.

event, so they can simply be neglected. In other words, the proton is *forced* to interact somewhere along the pathlength⁹ in the material, and any subsequent background events are *weighted* by the probability m that the proton which produced them *would* have interacted in the shield. This saves CPU time, at the expense of being rather confusing on a first glance.

In summary, N protons are picked isotropically on the sphere. Those whose trajectories intersect the telescope's shield are handed to FLUKA, which forces them to interact and follows their behavior, reporting the probability that each would have interacted if it were not forced. A certain number of the N protons, therefore, produce background events, and each background event is weighted by the probability that its originating proton would have interacted in the first place. If the background events are labeled by an index i , then the fraction of the N events that produced background events is

$$(\sum m_i)/N \quad (3.6)$$

and the actual background rate r_B is simply this fraction multiplied by the absolute rate¹⁰ at which protons hit the sphere, or

$$r_B = 0.9625 \frac{R^2 \sum m_i}{N} \text{ background events/s} \quad (3.7)$$

where R is the sphere's radius, the m_i are the weights of each background event, and N is the total number of protons incident on the sphere.

3.5.2 Extragalactic Diffuse Source

The signal produced by a source such as the extragalactic diffuse is somewhat simpler to calculate than that due to the cosmic-proton background. First some flux $J_{EG}(E)$ ¹¹ exposes the sphere¹², so the total incident rate on the sphere is $(8\pi^2)R^2J_{EG}(E)$. Of the trajectories exposing the sphere, a certain fraction 'a' will fall in the

⁹The point of interaction is chosen exponentially along the projection of the trajectory in the material

¹⁰cf. equation 3.3

¹¹Given by equation 3.1.

¹²cf. figure 3.1

aperature of the telescopes. The fraction 'a' is called the telescope's acceptance, and is defined relative to the specific choice of radius and position for the sphere. However, physical results are always independent of the choice of sphere, as will be demonstrated for the SAS-2 telescope in the next chapter. The extragalactic diffuse rate for a particular telescope model will be

$$r_{EG} = J_{EG}(E)(8\pi^2)R^2 \text{ gamma rays/s} \quad (3.8)$$

This is the total flux over an energy E.

3.6 Statistical Error Estimate

When two numbers are with unequal statistical weights are added, the one with a 'heavier' weight contributes more to the statistical error, e.g. if each number is obtained by a count, and the total count for both sets is N, then the total statistical error will actually be more than the Poisson result of $1/\sqrt{N}$. A useful formula for estimating the fractional error e for a sum of statistically weighted events is [10]

$$e = \frac{\sqrt{\sum m_i^2}}{\sum m_i} \quad (3.9)$$

which is convenient since if the m_i 's are all equal, it simplifies to the poisson counting result of

$$e = \frac{\sqrt{\sum m^2}}{\sum m} = \frac{\sqrt{N m^2}}{N m} = \frac{1}{\sqrt{N}} \quad (3.10)$$

and if the weights are not all equal, e is greater than the poisson result.

If there are two or more components which contribute to the sum, and they are due to a different numbers of incident protons, equation 3.9 requires modification. Instead of directly adding the sums of the weights and their squares, it is necessary to consider the relative exposures. This can be accomplished by replacing the weights m in 3.9 by each weight divided by its exposure N, and summing over all components. If one population is exposed to A protons and contains background events of weights a, and the other

is exposed to B protons and contains background events of weights b then the modified equation for the error estimate becomes

$$e = \frac{\sqrt{\sum(a_i/A)^2 + \sum(b_i/B)^2}}{\sum(a_i/A) + \sum(b_i/B)} \quad (3.11)$$

3.7 Discussion of Assumptions

The telescope model used in most simulations is rather simple¹³. The veto scintillator is assumed in all cases to be perfect, so that if a charged particle traverses any length of it, light will be emitted by ionization in the scintillating material and a veto signal received by the control circuits. The scintillators used in all telescopes considered are very efficient¹⁴ and this assumption is, in fact, strongly supported.

To simplify the physics of the background calculations, it was assumed that if a gamma ray passed through the converter layer and the bottom of the pair detector, the gamma ray was detectable. Taken at face value, this is not a good assumption since the conversion probability is generally around 30 percent, and then the effectiveness of the pair detector depends on the gamma ray's energy and trajectory. The most important results here, however, are relative comparisons between the cosmic-ray background and a reference diffuse flux, so that, as long as the same model is used to estimate the signal due to each, a good comparison can be made.

There are computer models of the pair detectors of several of the telescopes. The model of EGRET's spark chamber was used to compare a certain limiting case to accelerator tests. This model, combined with the FLUKA model of the cosmic protons and the shielding, provides a very comprehensive simulation of a gamma-ray telescope in the environment of outer space.

¹³cf. figure 1.1

¹⁴The EGRET veto scintillator, for instance, was designed so that it would miss no more than one trigger in a million [14]

Chapter 4

Several Case Studies

The mathematical methods and computer models described in the previous chapter were employed to characterize the cosmic-proton background in several gamma-ray telescopes. SAS-2, EGRET, and GRITS have been analyzed in this way, and the results detailed here are summarized in Appendix C. Differential spectra of the proton-induced background is given for each of the telescopes in Appendix B. It is important to note that the spectra are only approximate because the total number of background events in each bin is quite small. Pictures and diagrams of the telescopes are given in Appendix A.

The benchmark source for all background calculations will be the extragalactic diffuse source 3.1

$$J_{EG}(E) = 6.7 \times 10^{-3} E^{-1.35} \text{ gammas/cm}^2\text{s sr} \quad (4.1)$$

For a practical comparison between this source and a background, it is necessary to choose an energy E over which to calculate it. Any realistic telescope will have a lower threshold under which it is ineffective in detecting gamma rays. This threshold is of usually around 100 MeV, so the comparison that will be made will be ratio of the cosmic-proton background signal over 100 MeV to the extragalactic diffuse signal over 100 MeV. The extragalactic diffuse flux over 100 MeV is

$$J_{EG}(100 \text{ MeV}) = 1.34 \times 10^{-5} \text{ gammas/cm}^2\text{s sr} \quad (4.2)$$

4.1 The SAS-2 Telescope

The SAS-2 gamma-ray telescope was orbited by NASA in the early 1970's. Its gamma-ray detector is based on two spark chambers. The converter is located in the top spark chamber and is composed of thin plates of tungsten located between the layers of the spark chamber. There are two scintillators in the detector, one between the spark chambers and one at the bottom of the telescope. An event is counted only if both of these scintillators are triggered by the electron/positron pair. The spark chamber's field of view is a square 25 cm on a side, or 625 square centimeters. The veto scintillator is dome-shaped and completely surrounds the telescope. The thermal shielding is located directly outside the veto scintillator.

4.1.1 The Telescope Model

As discussed in section 3.7, the analysis routines of the computer model assume that a gamma ray is acceptable if its trajectory passes through the telescope's aperture. In the SAS model, the telescope's aperture is modeled by two square hodoscopes¹ which represent the two scintillators mentioned above. This model obviously accepts far more gamma rays than the actual telescope would since its angular aperture is wider and no account is taken of the probability that a gamma ray will not interact in the converter². There is a difference, though, between a gamma ray which has been detected and one which is detectable. Any gamma ray which passes both hodoscopes is, in theory, detectable, so that it should be recorded. If a realistic result, such as a count rate which can be compared to a real experiment, is needed, a model of the spark chamber can be used to determine the probability that each trajectory would result in a detected gamma ray. This is done in the final case study to predict the results of an EGRET calibration in a beam test. It is not necessary, however, to use a model of the spark chamber if a comparison of two signals is sought, i.e. a comparison of the background versus the extragalactic diffuse.

¹Jargon term for a shape through which a trajectory is required to pass

²Usually less than a third of the gamma rays interact in the converter.

Component	Density g/cm ³	Thickness cm	Amount of Material gm/cm ²
Fiberglass Dome	5.24	0.038	0.20
Thermal Blanket	0.15	0.95	0.15
Total	—	—	0.35

Table 4.1: Materials in the SAS-2 thermal shield

4.1.2 The Shield Model

The SAS-2 shield is composed of two layers³. There is a fiberglass layer located flush to the veto scintillator dome and a thermal blanket surrounding it [11] [12]. Their densities and thicknesses are listed in table 4.1.2.

The thermal blanket has two geometrically distinct parts. Calculations have been done for one of these parts, but the geometry of the other part is complex, rendering the computation intractable thus far. It was possible, however, to estimate its contribution to the background rate by noting that it subtends approximately 1.3 times as much solid angle in the telescope's aperture as its companion does, so its presence can be accounted for by simply multiplying the contribution of the thermal blanket by a factor of $1+1.3=2.3$.

Exact figures were unavailable for the actual atomic compositions of the shield layers. The shield composition was approximated by carbon, since this element is common in the plastics which compose the shield. Since the shield consists of two layers, a separate calculation was done for each, and the results were added. This is justified by the fact that the probability that a given proton will interact in one layer is of the order of a percent so that the probability that the same proton will interact in both shield layers is of the order of 0.01 percent, or negligibly small.

4.1.3 Extragalactic Diffuse Count Rate

For each of the telescope models, the extragalactic diffuse count rate was computed by exposing the sphere⁴ to isotropic trajectories

³cf. Appendix A

⁴cf. figure 3.1

and counting the fraction that intersected both hodoscopes of the detector model. This fraction was then multiplied by the total area exposed to the flux⁵ and the absolute flux 4.2. The calculated rate is given by equation 3.8 to be

$$r_{EG} = 0.00631/s \quad (4.3)$$

It was found that this method was independent of the size and offset of the sphere, and that with sufficient calculation time⁶ the statistical fluctuations of the monte carlo integral could be reduced to the order of a percent. The total statistical error of each background measurement is therefore taken to be purely due to the background calculation itself.

Physical results must be independent of the size of the sphere used; if this were not true, this method of choosing random trajectories could not be used. Since the two shield components of SAS-2 had different geometries, spheres of different radii were chosen for the two simulations. The radius of the sphere chosen for the fiberglass layer was 40 cm, that for the thermal blanket 45 cm. Each was then calculated to have a different acceptance⁷. That for the fiberglass dome was found to be 0.003727, that for the thermal blanket 0.002944. When substituted into equation 3.8, these give identical numbers, or provide an example of the fact that physical calculations cannot depend on the exact configuration of the sphere.

4.1.4 Background Estimate

The SAS-2 telescope did not follow an orbit identical to that planned for GRO, but rather one closer to the equator. Therefore the Earth's magnetic field shielded SAS-2 somewhat more than it will shield GRO, resulting in a smaller total flux than is represented in figure 2.3. The same spectrum was used for the simulation SAS-2 as for that of EGRET, however, rendering the background estimate conservative.

⁵i.e., the sphere's surface area

⁶i.e., requiring 10,000 accepted trajectories out of some hundreds of thousands

⁷cf. section 3.5.2

Shield Component	N	$\sum m_i$	$\sum m_i^2$	e, percent	r_B , events/s
Fiberglass dome	364067	0.05736	0.001228	61	0.000243
Thermal blanket	550443	0.04959	0.0002600	33	0.000176

Table 4.2: Calculated quantities for the SAS telescope model

Note that the comparison here is intended to reflect the ratio of the background rate to the extragalactic diffuse rate for a telescope with a gamma-ray detection threshold, so that the background rate here and in the next two case studies corresponds to the background rate for gamma rays whose energies are greater than 100 MeV.

The background rate is given by equation 3.7, and the fractional error by equation 3.9. The quantities that are required to compute the rate and its statistical error are N , $\sum m_i$ and $\sum m_i^2$. The results for the two components of the shield are given in table 4.1.4.

There is a third component to the SAS-2 thermal shield which has a relatively complex geometry but is similar in composition to the thermal blanket layer. It subtends approximately 1.3 times as much solid angle of view as the thermal blanket layer does, so its contribution to the background rate is approximated by 1.3 times that of the thermal blanket.

The individual contributions to the background rate can be added to yield a total rate but equation 3.11 must be used to combine the errors since the number of protons exposing each shield layer is different. The total background rate is

$$r_B = 0.000648/s \quad (4.4)$$

with an error estimate of 31 percent. The ratio of the proton-induced background to the extragalactic diffuse signal is then 0.103 ± 0.03 .

4.2 The EGRET Telescope

The EGRET⁸ telescope is scheduled to be flown aboard the GRO spacecraft in late 1990. Its design is similar to that of SAS-2 although it is much larger. Its spark chamber has a square field of

⁸Energetic Gamma-Ray Experiment Telescope

Component	Density g/cm ³	Thickness cm	Amount of Material gm/cm ²
Inner Layer	0.1182	1.0	0.1182
Outer Layer	0.0194	2.54	0.0493
Total	—	—	0.1675

Table 4.3: Materials in the EGRET thermal shield

view, 80 cm on a side, an area of 6400 square centimeters. This collecting area is a factor of ten larger than that of SAS-2, and hence will allow EGRET to pinpoint sources far better. In addition to the spark chamber, EGRET has a NaI crystal scintillator calorimeter which absorbs the pair and measures their energy. Proper calibration of this device allows an estimation of the gamma ray's energy.

EGRET's mission is quite ambitious. Since NASA hopes to operate GRO for at least several years, EGRET will be used to make a detailed map of the gamma-ray sky. Although its angular resolution is not much larger than that of SAS-2, its larger collection area will allow the detection of much weaker point sources and much fainter variations or details in the diffuse sources.

4.2.1 The Telescope Model

Since EGRET is quite similar in design to SAS-2, its model is identical in concept to that of SAS-2. A single sphere of radius 110 cm was used to simulate both shield layers, and the acceptance with respect to that sphere was 0.005545.

4.2.2 The Shield Model

EGRET's thermal blanket consists of two layers, one denser than the other. Both layers are composed primarily of Carbon, Oxygen and Nitrogen in the approximate ratio 67:24:9. The densities and thicknesses of the layers are given in table 4.2.2.

4.2.3 Extragalactic Diffuse Count Rate

The extragalactic diffuse count rate for the EGRET model is given by equation 3.8

$$r_{EG} = 0.0710/s \quad (4.5)$$

4.2.4 Background Estimate

The data required to calculate EGRET's background rate is presented in table 4.2.4. The total background rate is

$$r_B = 0.00531/s \quad (4.6)$$

with an error of 31 percent. The ratio of the background to the extragalactic diffuse is then 0.040 ± 0.012 . This is consistent with an early estimate [14] which claimed that (the thermal shielding) "will generate a gamma-ray background (>100 MeV) equivalent to less than eight percent of the celestial diffuse flux for 85 percent of the orbit and less than three percent for 50 percent of the orbit". At this time, EGRET's design specifications included only half the inert material, i.e. 0.08 gm/cm^3 that will actually be included. It can be concluded that this initial estimate was conservative; if the density in the EGRET shield model were halved, then so would the background rate. The current prediction could then be that the background will be '2 percent of the extragalactic diffuse flux for 100 percent of the orbit.' It is in the nature of estimations, though, that they be cautious so it is evident that the current calculation of EGRET's background is in good agreement with the earlier estimate.

It is easily seen that the proton-induced background must be proportional to the amount of material in a telescope's shield. SAS-2 has about 2.2 times as much material in its shield (per unit area, of course) as does EGRET. Furthermore, the model's prediction for SAS-2's background is about 10.2 percent of the rate predicted for the extragalactic diffuse flux. EGRET's background is only about 4 percent of the extragalactic, so in terms of background relative to the extragalactic diffuse source, SAS-2 is about 2.5 times worse than EGRET. This supports notion that a telescope's proton-induced background is proportional to the amount of material in its shield quite well.

Shield Component	N	$\sum m_i$	$\sum m_i^2$	e, percent	r_B , events/s
Inner Layer	525863	0.08226	0.001401	46	0.00189
Outer Layer	462458	0.03904	0.0001287	29	0.000983

Table 4.4: Calculated quantities for the EGRET telescope model

4.3 The GRITS Telescope

The GRITS telescope has been proposed by NASA [1]. It will be constructed in the discarded external fuel tank of the space shuttle⁹. The telescope's aperture will be oriented through the bottom of the tank. Its detector will employ the Cerenkov scheme¹⁰; the Cerenkov gas will occupy most of the inside of the tank. The converters and veto scintillators will be combined into small hexagonal packages, and then arranged across the aperture of the telescope according to one of several possible configurations. The aperture of the telescope will cover most of the cross section of the tank, which has a radius of 420 cm, so the total collecting area will be about 550,000 square centimeters, nearly one hundred times larger than that of EGRET and one thousand times that of SAS-2. With this much collecting area, GRITS will be able to locate sources quite accurately. Its energy resolution will not be nearly as good as EGRET's, since a calorimeter large enough to cover the back of the telescope would be far too heavy to be feasibly included. The main goal of GRITS is, therefore, to locate point sources precisely enough to identify them with sources in other wavelengths.

4.3.1 Telescope and Tank Wall Models

The telescope's pair detector is modeled by two circular hodoscopes, one at the top and one at the bottom of the tank; these define a cylinder which roughly corresponds to the tank's cylindrical volume. The tank wall is made of Aluminum ($\rho = 2.7 \text{ gm/cm}^3$) and is 2 mm thick so it presents 0.54 gm/cm^2 to normal trajectories. Its shape is approximated by a spherical section which is chosen so as

⁹cf. Appendix A

¹⁰cf. section 1.2

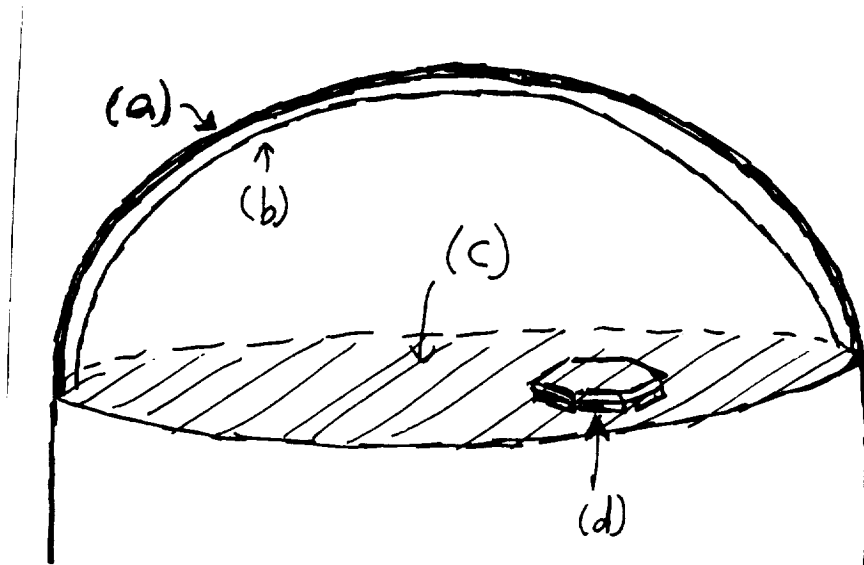


Figure 4.1: Three possible arrangements for the converter/veto scintillator packages in GRITS. (a) Flush to the tank wall. (b) Offset from the tank wall by one inch. (c) Planar below the tank's end cap. (d) A converter/veto scintillator package.

to correspond to the locations of the true shape at the tip and at the edges. Concerns about the astronauts' safety have motivated the consideration of several different designs for the converter and the veto scintillator.

4.3.2 Three Possible Configurations

Since GRITS must be assembled in orbit, the specifics of its design must be very modular; it must be easy for astronauts to assemble. The veto scintillator and converter will therefore be combined into small hexagonal packages, and these packages will form a patchwork over the aperture of the telescope. There are several ways in which these packages could be arranged, as is shown in figure 4.1.

The ideal arrangement would place the packages flush against the tank wall. The closer the veto scintillators are to any inert material, the better the chance that they will detect any charged

Configuration	N	$\sum m_i$	$\sum m_i^2$	e, percent	r_B , events/s
Flush	674258	0.2077	0.01649	62	0.0741
Offset 1 inch	460249	0.05817	0.001399	64	0.0304
Planar	462496	1.071	0.03978	19	0.577

Table 4.5: Calculated quantities for the GRITS telescope model

secondaries of proton interactions.

A more realistic version of this arrangement places the packages one inch off the wall; this allows for fastenings, curvature variations and light tube assemblies to take the scintillator light to photomultiplier tubes.

The simplest design, and hence the safest for the astronauts to assemble, would place the packages in a flat disk at the aperture end of the telescope, i.e. exactly where the front hodoscope lies in the detector model. This would place it fairly far from the front tank wall, so many more charged secondary particles would be able to escape detection by the veto scintillators.

4.3.3 Extragalactic Diffuse Count Rate

The sphere used to expose GRITS to isotropic fluxes had a radius of 500 cm, and a geometrical acceptance of 0.003785. Now, the space shuttle's fuel tank is clearly large than a sphere of radius 500 cm. The tank is large enough to contain the Wright brothers' whole first flight! The sphere need not contain the whole telescope, however. The only material that it must include, in fact, is that portion of the tank wall which is directly within the telescope's aperture. With this sphere and acceptance, the extragalactic diffuse source count rate is given by equation 3.8

$$r_{EG} = 0.999/s \quad (4.7)$$

4.3.4 Background Estimate

Then the ratios of the background to the extragalactic diffuse for each arrangement are: Flush 0.07 ± 0.05 , Offset 0.03 ± 0.02 , and Planar 0.56 ± 0.11 . The first two arrangements then produce background signals which are identical within statistical errors and the

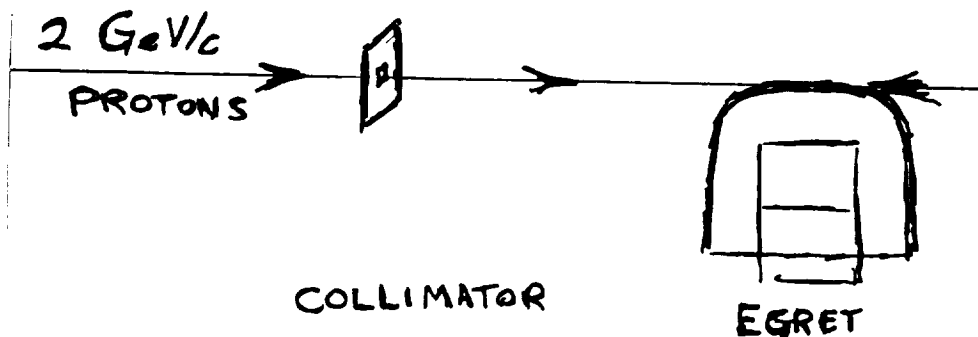


Figure 4.2: Configuration of the EGRET beam test at Brookhaven. Protons exposed the shield and background gamma rays were counted.

planar configuration produces a signal which is similar in intensity to the extragalactic diffuse.

It should be noted that, since the primary mission of GRITS is to locate point sources precisely, the proton-induced background is not so serious a threat as it is to EGRET, whose mission is to survey both diffuse and point sources.

There are two conclusions which can be drawn from these results. First, if it is desired that the proton-induced background be negligible as compared to the extragalactic diffuse signal, both the flush-mounted and the offset arrangements will suffice. Second, if it is decided that astronaut safety is paramount, the background produced will not cripple the telescope, but will only increase the inherent background slightly.

4.4 Beam Test of EGRET

The EGRET telescope was placed in a beam at Brookhaven National Laboratory and exposed to protons incident from several trajectories. One of these was chosen as an experimental result against which the computer model of EGRET could be judged. The trajectory grazes the top of the thermal shield, illuminating a rectangular cross section, as shown in figure 4.2 The beam was collimated by placing a plastic scintillator, which had a rectangular

hole punched out, upstream of the telescope; a trigger in this scintillator would veto any event subsequent events in the telescope.

The fraction of the protons which produced gamma rays acceptable by the telescope was estimated to be in the range [13]

$$f_{\text{est}} = (0.3 - 2.6) \times 10^{-6} \text{ gammas/proton} \quad (4.8)$$

This estimate includes beams of momenta of 2, 5 and 9 GeV/c. It was found that the fraction f did not depend significantly on the beam's momentum.

4.4.1 Beam Test Model

Each Brookhaven proton beam was roughly monoenergetic and distributed uniformly over a rectangular cross section, so the calculation of the incident protons' trajectories was greatly simplified. An additional simplification resulted from the fact that the beam was oriented at a grazing incidence on the shield. First, for this type of trajectory, there is a large path length in the material and hence a large chance that a given proton will interact. Furthermore, since most secondaries of a nuclear interaction will be moving in the beam direction, many of the interactions will escape veto by the detection of charged secondaries. There are a significant number, therefore, of detectable gamma rays per incident proton, so the protons' nuclear interactions need not be forced and the statistical weighting of subsequent events need not be performed.

The comparison desired here is not between two computer models of detected signals, but between a model and an experiment. It is necessary, therefore, to treat the telescope in a more detailed manner. The calculation is broken down into two steps. The first approximates the telescope with two square hodoscopes, as in the previous EGRET simulation. The second step uses a computer model of the detector which is constructed around the EGS¹¹ code. The spark chamber model is maintained and was operated by Y. C. Lin [16]. The computer model takes a gamma-ray trajectory and energy and computes a probability that the telescope will detect it. The sum of the probabilities estimates the number of gamma

¹¹Electron-Gamma Shower [15]

rays that would have been detected. An error can be obtained from equation 3.9.

4.4.2 Estimated Rate of Acceptable Gamma Rays

The incident protons were given a momentum of 2 GeV/c, and 400,000 were used in the simulation. Of these, 35 produced unvetted gamma rays whose trajectories intercepted both hodoscopes. These 35 gamma ray trajectories and their corresponding energies were then passed to the spark chamber model, which gave a probability that each gamma ray would interact. The sum of these probabilities is $\sum m_i = 7.02$; the average probability is then $7.02/35=0.20$; the average detector efficiency was twenty percent for the gamma rays. The sum of the squares of the probabilities was $\sum m_i^2 = 1.65$ so that the statistical error of the simulation¹² is about 18 percent. Then the estimated probability, per proton, that an unvetted gamma ray will be detected is

$$f_{\text{model}} = 1.8(\pm 0.3) \times 10^{-6} \text{ gammas/proton} \quad (4.9)$$

This fraction is nearly an order of magnitude higher than that from the analysis of beam test data, equation 4.8. The discrepancy may have arisen because certain steps were neglected in the analysis of the gamma rays. The most important of these steps is the actual analysis of the spark chamber tracks. In practice, the spark chamber tracks are interpreted by hand, and a significant fraction may not be identifiable as events. Further communication is underway to determine the source of the difference.

If, in fact, the telescope models do predict background rates that are higher than are really observed, there will be no cause for alarm since the same models predict that the cosmic background in orbit will not overwhelm interesting sources. The background predictions for the EGRET and GRITS telescopes would then have to be reduced from their current values!

¹²cf. equation 3.9

Chapter 5

Conclusions and Context

The trend in the sizes of gamma-ray telescopes has obeyed the usual law of the growth of physics experiments — ‘make the next one bigger!’. Several decades ago, balloon-borne telescopes ascertained the existence of gamma-ray sources from outer space, and a series of ever-larger telescopes followed.

5.1 The Advance of Gamma-Ray Astronomy

COS-B, although limited by the very background discussed in this report, was able to assemble the first gamma-ray map of the sky. SAS-2 was designed to minimize this background, so was able to make a more detailed survey. One aspect of this survey was an estimate of the extragalactic diffuse source’s spectrum. The model presented here supports this estimate first by showing that the proton-induced background for SAS-2 was only ten percent as strong as the extragalactic diffuse signal. Second, the cosmic-proton background’s spectrum is characterized for the one model in Appendix B, and is compared in shape to that of the extragalactic source. The shapes are quite different, so the observation of a power-law spectrum strongly supports the hypothesis that it really is a genuine source, not simply an instrumental anomaly.

When it is launched later this year, EGRET will begin making the most detailed map of the gamma-ray sky to date. Since its collecting area is an order of magnitude greater than any previous

gamma-ray telescope, EGRET is expected to uncover many undiscovered weak point sources, as well as reveal yet unseen structure in diffuse sources such as the galactic center, or variations in the extragalactic diffuse source. A high proton-induced background would increase the observing time required to locate weak point sources and also limit the amount of structure observable in diffuse sources. The computer model of EGRET presented here indicates that this background would be less than 4 percent of the strength of the weakest diffuse source, the extragalactic diffuse. This computation is supported by a comparison with a beam test of the EGRET telescope, in which the computer actually predicted a higher background than was observed in the telescope. Even early estimates placed the background below the level of the extragalactic diffuse for EGRET, but none carries the rigor of deducing the background from observed cosmic-ray characteristics and basic physical laws.

If built, the GRITS telescope will provide the logical next step in the evolution of gamma-ray telescopes. With two orders of magnitude more collecting area than EGRET and three more than SAS-2, GRITS will have an unparalleled ability to locate gamma-ray sources, enabling them to be identified with known sources of other wavelengths of radiation. Thus far, only three of the twenty some-odd sources have been positively pinned to visible objects, two pulsars by their time variation and one dense cloud due to its fortuitous lack of near neighbors. A large background due to cosmic-ray protons interacting in the GRITS tank wall would increase the length of time required to pinpoint sources, and hence would decrease the amount of information obtainable in the telescope's lifetime. However, there is diffuse radiation coming from all directions; this is the weakest out of the galactic plane, i.e. from the extragalactic source. When fixing on a point source, this diffuse radiation counts as a background. By predicting that for all three of the potential GRITS designs the background is a fraction of the weakest natural background in the sky, it is shown that the proton-induced background will in no way affect GRITS adversely in its mission of locating point gamma-ray sources.

5.2 Applicability to Similar Fields

For a number of years, high-energy physicists have employed monte-carlo computer programs to predict and interpret accelerator experiments. The origin of the two monte carlo codes used here, FLUKA and EGS, is the experimental high-energy physics community. These computer codes have proven their grit by using observed and inferred physical relations to predict new phenomena, as well as providing vehicles by which to test complex predictions of modern particle theories. The availability of such powerful new computer tools has actually spawned a new branch of high-energy physics, called phenomenology, which is located somewhere in between theory and experiment, and provides the calculational bridge when a complex experiment or abstruse theory causes a rift between the two extremes.

Ideas of particle phenomenology can be applied well to any sort of astronomy in space. It is difficult to test a satellite's behavior without launching it, and that is of course too late to begin testing. With the modern breadth of data on the cosmic-ray environment, and the relative completeness of current physical description at most cosmic-ray energies, monte carlo calculations such as those presented here offer a very versatile theoretical tool in evaluating the effects of an orbital environment on any sort of telescope.

The results presented in this report and their agreement with both experiment and common sense indicate that large monte carlo codes such as FLUKA that attempt to incorporate a comprehensive description of medium- to high-energy physics are a powerful tool for predicting the behavior of any orbiting system.

Aside from the obvious applications to telescopes which operate in space at other wavelengths, these codes could be employed in accurately predicting and interpreting the results of Extensive Air Shower measurements. These showers are caused by cosmic rays or gamma rays with very high energies. A detailed calculation of the observable shower characteristics would enable ground-based astronomers to better determine the nature of the initiating radiation.

5.3 Future Work in Gamma-Ray Astronomy

GRITS is the largest telescope that could conceivably be constructed in Earth orbit, but even it has a limited angular resolution. One possible next step would be a telescope located on the surface of the moon. This telescope could have a very large collecting area, and it could obtain a very precise measurement of a source's position by watching as it extinguishes on the horizon, i.e. as it sets [17]. Since the moon's does not have a strong magnetic field to shield its surface from cosmic rays, the cosmic-proton flux is attenuated only by the solar wind. The moon's surface would therefore have a very large 'gamma-ray albedo', in analogy with the visible reflectivity of other planets. This albedo would obscure the true horizon, and hence the setting of the interesting source, for sources below a certain strength. A calculation of the absolute rate of this albedo has been performed using FLUKA, and a limiting form for the emission at small angles, i.e. at the horizon is now in the process of being derived.

There are a number of FLUKA-equivalents espoused by different groups and institutions. A competitor at CERN is called GEANT, one at Los Alamos National Laboratories is called HETC, etc. These are all constructed on different models, so it would be instructive to examine the background calculations for model-dependence. Work may begin this summer to check HETC, and inquiries are being made about GEANT.

Appendix A

Pictures of the Real Telescopes

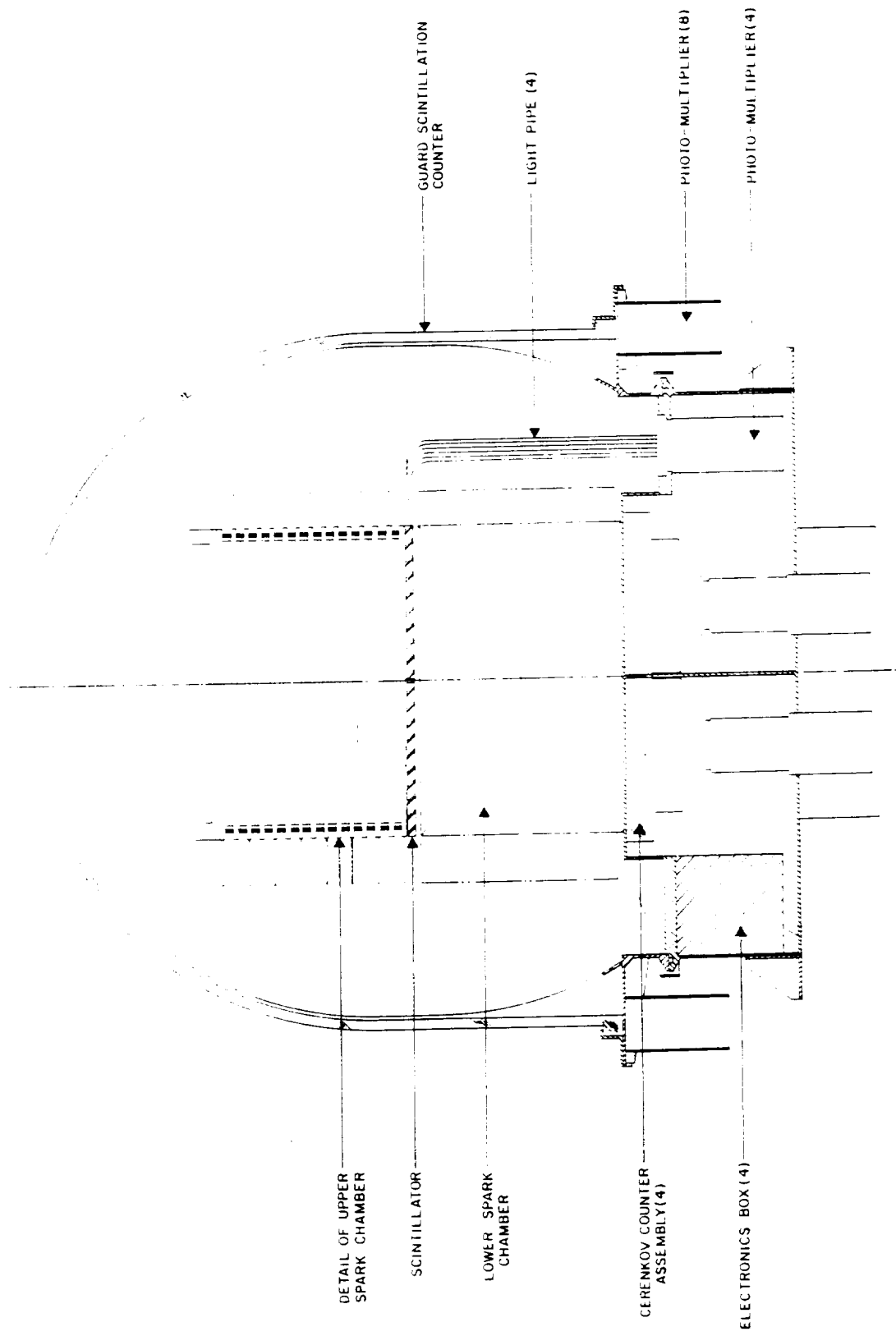


Fig. 1. A schematic diagram of the SAS-B digitized spark chamber gamma ray telescope

ORIGINAL PAGE IS
OF POOR QUALITY

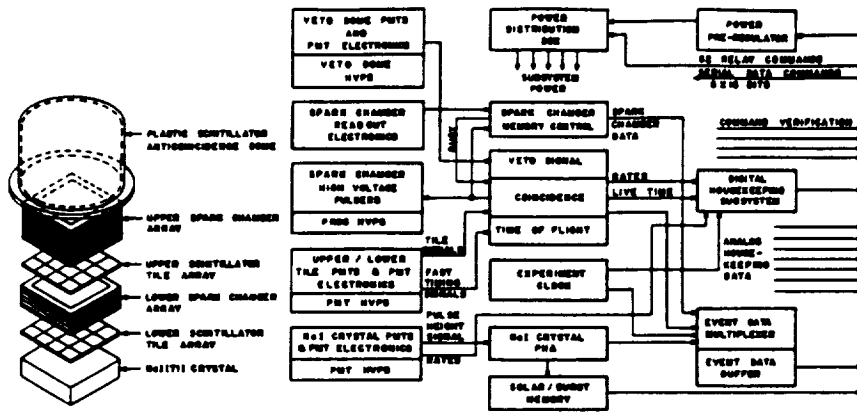


Fig. 2 A block diagram of the instrument electronics.

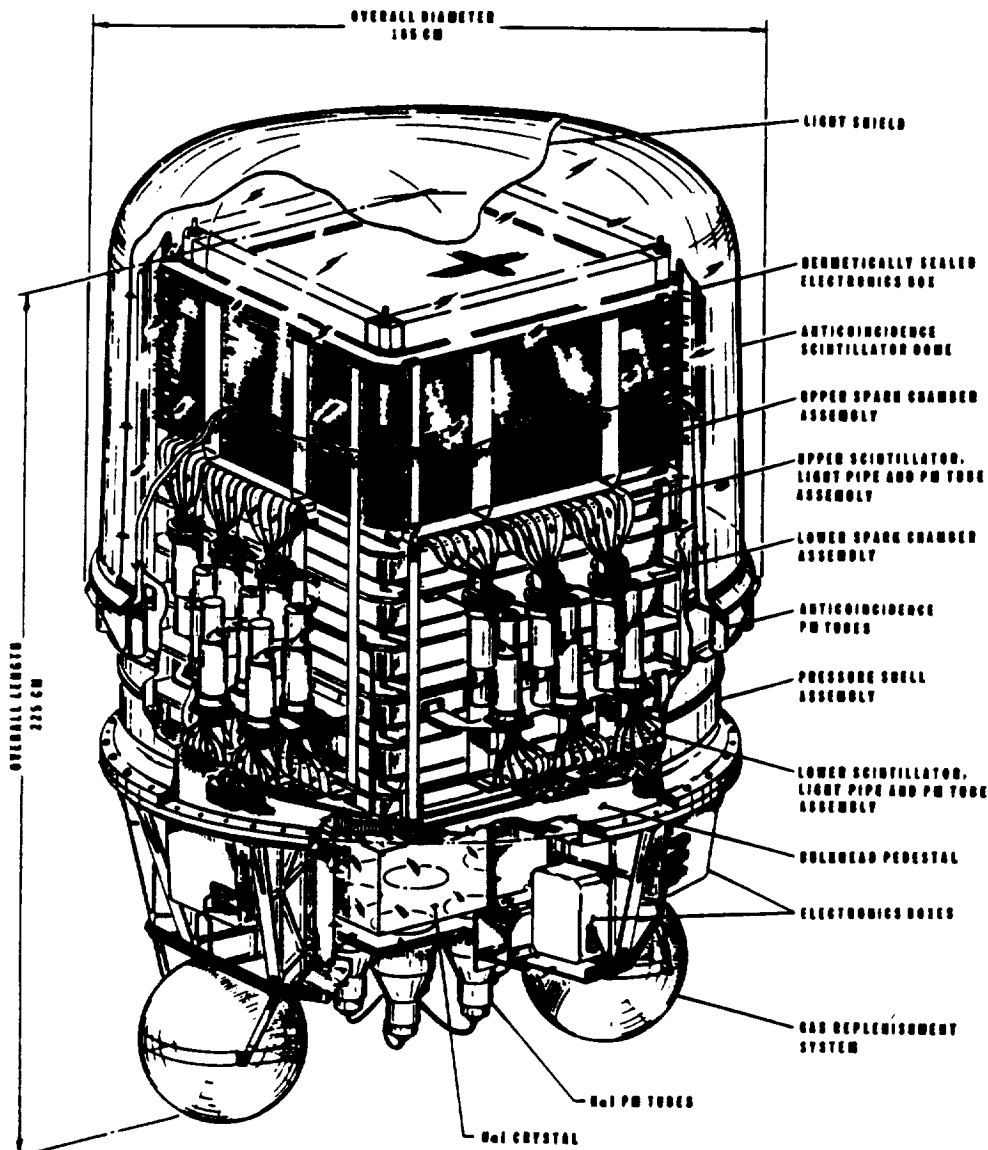


Fig. 3 An isometric drawing of the high energy Y-ray telescope.

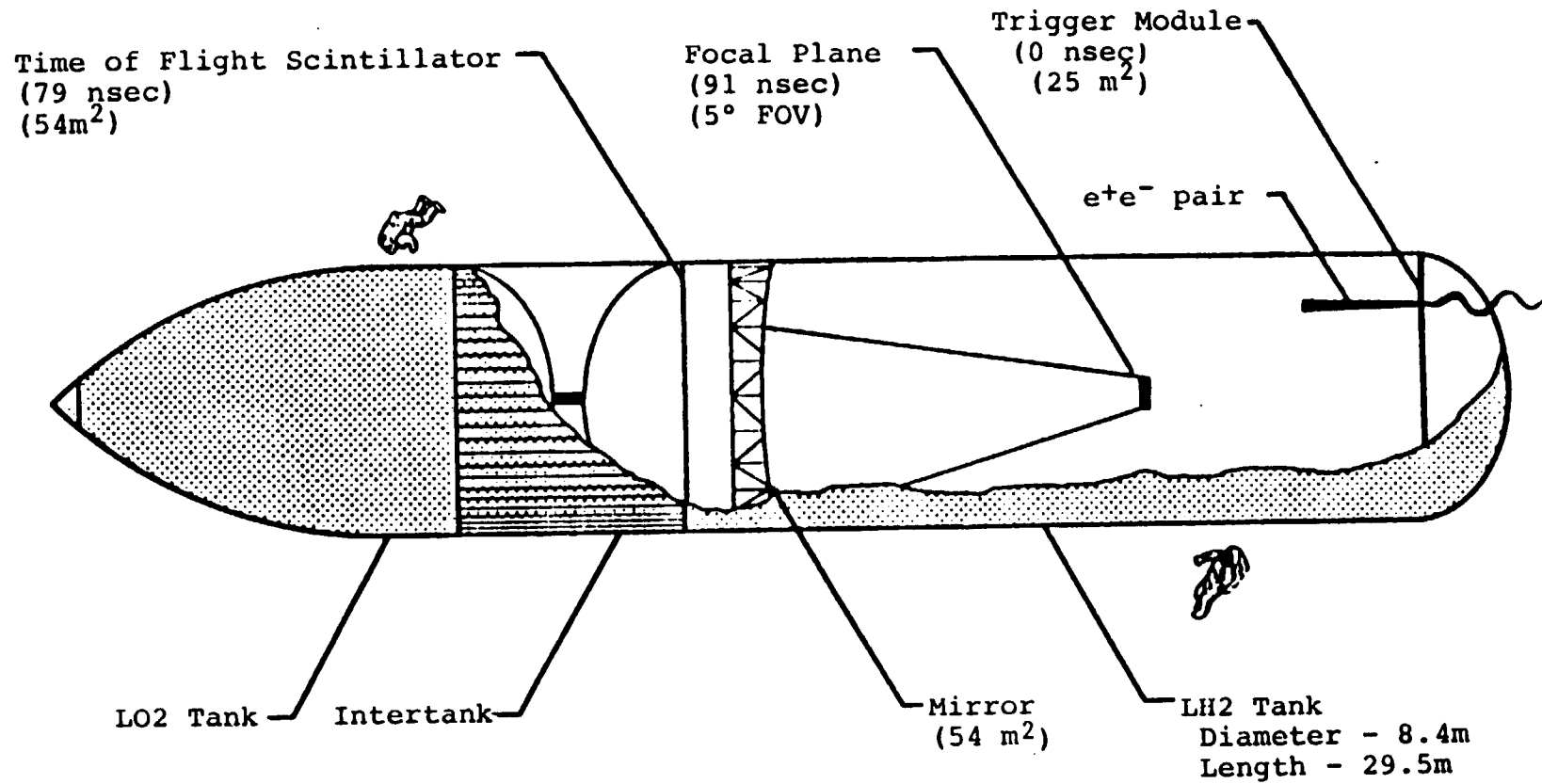


Figure 1 Schematic of The Gamma-Ray Imaging Telescope System (GRITS).

Appendix B

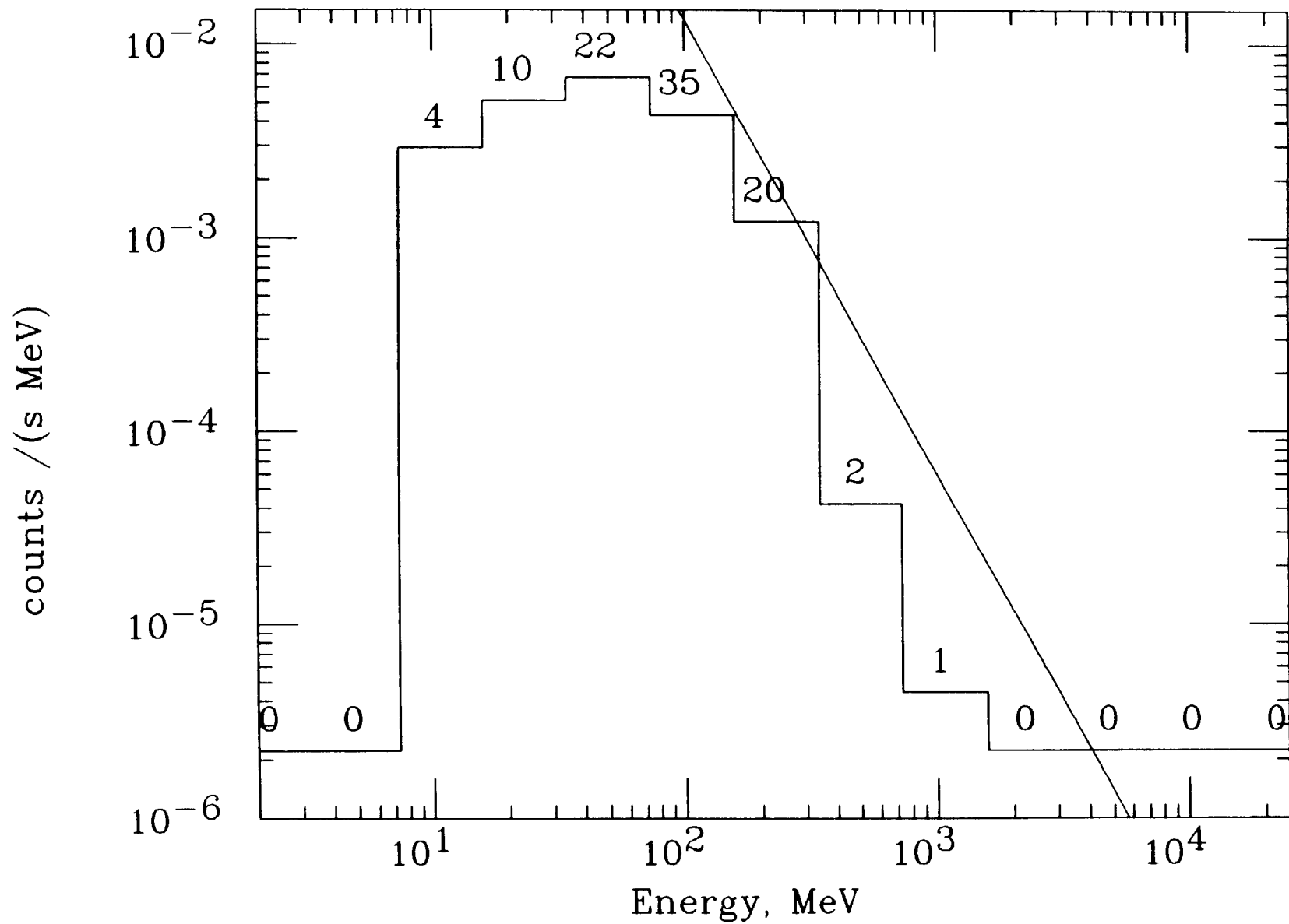
Background Spectrum from a GRITS Model

The background spectrum presented here is from the GRITS model with the planar converter/veto scintillator package arrangement. The number of background events in each bin is printed above each bar; as can be seen, the number of counts per bin is often quite low. For other models, the number of background events obtained was even smaller, so that their spectra were even sketchier. However, they generally display the same shape; this shape characterizes the physics of their production mechanism.

When a π^0 decays, it produces two 67.5 MeV gamma rays in its rest frame. When the π^0 decays in motion, the gamma rays will be either red-shifted or blue-shifted, depending on whether they are emitted opposite the direction of the π^0 's motion or with it. Since the proposed mechanism for the proton-induced background is π^0 decay, spectra of this background should be peaked near 70 MeV and fall off evenly on each side.

The actual spectra deviate slightly from these expectation simply because all cosmic-ray protons are incident from outside the detector, so the π^0 's are emitted preferentially toward the telescope and hence more gamma rays are blue-shifted than are red-shifted.

Background and E-G Spectra for GRITS



Appendix C

Summary of Background Estimates

Each telescope model is surrounded by a sphere of radius R which is used to obtain an isotropic exposure of a desired flux. If trajectories are picked randomly on this sphere, then a certain fraction 'a' will be within the telescope's aperture, as defined by the model. When considering an isotropic flux of gamma rays, a signal can be predicted quite readily. For instance, the flux of gamma rays with energies over 100 MeV in the extragalactic diffuse source is

$$\phi = 1.34 \times 10^{-5} \text{ gammas/cm}^2 \text{ s sr} \quad (\text{C.1})$$

The count rate in the telescope due to this source is then given by the equation

$$r_{EG} = \phi(4\pi(R \text{ cm})^2)(2\pi \text{ sr})a \text{ gammas/s} \quad (\text{C.2})$$

The values of R , a and r_{EG} are tabulated in table C.

Telescope	Component	R, cm	a	r_{EG} , /s
SAS-2	Fiberglass	40	0.003727	0.00631
	Thermal Blankets	45	0.002944	0.00631
EGRET	both	110	0.005545	0.0710
GRITS	all	500	0.003785	0.999

Table C.1: Extragalactic diffuse count rates for the telescope models.

Telescope	Component	N	N _B	$\sum m_i$	$\sum m_i^2$
SAS-2	Fiberglass	364067	8	0.05736	0.001228
	Thermal Blanket (i)	550443	12	0.04959	0.0002600
	Thermal Blanket (ii)	550443	12	0.06447	0.0004394
EGRET	Inner	525863	12	0.08226	0.001401
	Outer	462458	19	0.03904	0.0001287
GRITS	Flush	674258	5	0.2077	0.01649
	Offset	460240	4	0.05817	0.001399
	Planar	462496	57	1.071	0.03978

Table C.2: Data needed to calculate the background rates of the different telescopes.

To compute the background rate for a given model, N protons are distributed isotropically and homogeneously about the reference sphere. Some of these intersect the telescope's shield, and so have a probability m of undergoing a nuclear interaction. To save computer time, all are forced to interact and any subsequent background event is weighted by the probability that the proton would have interacted. The total proton flux is the integral of the spectrum of cosmic protons in Earth orbit, given in chapter 2:

$$\Phi = 0.01219 \text{ protons/cm}^2 \text{ sr} \quad (\text{C.3})$$

The total background rate is then given by the product of the sphere's exposure and the fraction of that exposure that gives rise to a background event:

$$r_B = \Phi(4\pi(R \text{ cm})^2)(2\pi \text{ sr}) \frac{\sum m_i}{N} \text{ events/s} \quad (\text{C.4})$$

If just one population, i.e. shield model, gives rise to the background, the error can be estimated by equation 3.9. If more than one population is involved, then equation 3.11 and its generalization to 3 and more populations must be used. The background rates and calculations leading up to them are recorded in tables C and C. N_B is the actual number of incident trajectories that led to background events.

Telescope	Component	r_B , /s	e, percent	r_B/r_{BG}
SAS-2	both	0.000648	31	0.103
EGRET	both	0.00287	30	0.0404
GRITS	Flush	0.0741	62	0.074
	Offset	0.0304	64	0.030
	Planar	0.557	19	0.56

Table C.3: Comparison of background to extragalactic diffuse rates for the different telescope models.

Bibliography

- [1] report prepared for NASA by D. Koch et al, *High Energy Gamma-Ray Measurements in the Space Station Era* (October 1987) Prepared at Smithsonian Institution Astrophysical Observatory
- [2] Beuermann, *Journal of Geophysical Research* 76, 4292 (1971)
- [3] Hayakawa, *Cosmic Ray Physics*. Wiley Interscience (1969) p. 563
- [4] Sandstrom, *Cosmic Ray Physics*. New York, Wiley and Sons (1965) p. 352
- [5] Sandstrom, p. 373
- [6] Sandstrom, pp. 4-5
- [7] Sandstrom, pp. 372-373
- [8] Thompson and Fichtel, *Astron. Astrophys.* 109, pp. 352-354 (1982)
- [9] Aarnio et al, *FLUKA86 User's Guide, CERN Divisional Report TIS-RP/168* (1986)
- [10] Bevington, *Data Reduction and Error Analysis for the Physical Sciences*. McGraw-Hill (1969)
- [11] C. Fichtel, private communication
- [12] R. Hartman, private communication
- [13] R. Hartman, private communication

- [14] Thompson et al, *IEEE Transactions on Nuclear Science*. 27, 364 (1980)
- [15] W. R. Nelson, et al, *The EGS4 Code System*. SLAC Report 265. December 1985
- [16] Y. C. Lin, private communication
- [17] D. Koch, private communication